Chapter 8

Luminescent Transition Metal Complexes as Optical Sensor for Cu (II) and DNA.

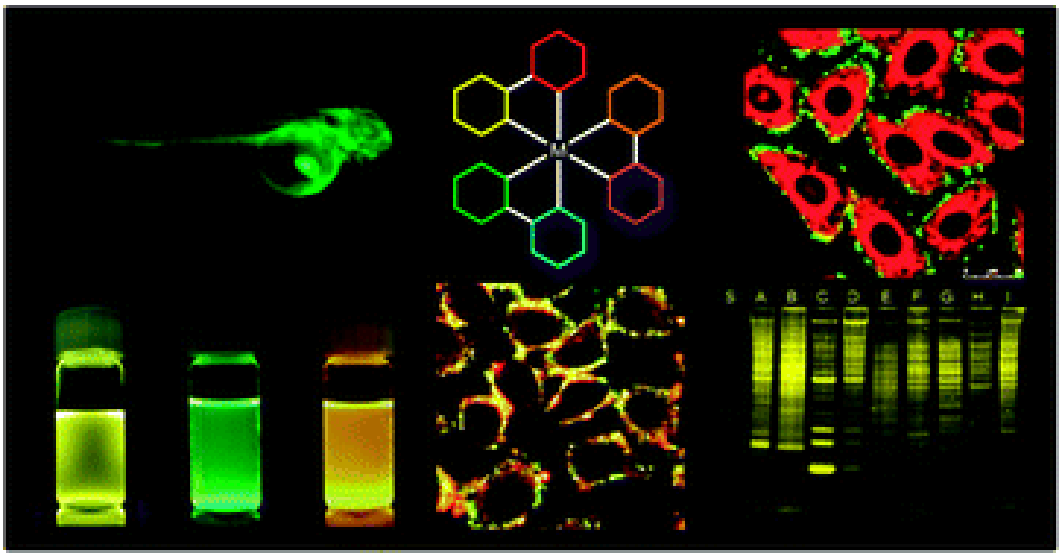

8.1 Introduction

Luminescent metal complexes have attracted increasing attention in the literature over the last few decades. Spearheaded by pioneering developments in ligand field theory and in the understanding of electronic transitions and spectroscopy of transition metal complexes, these compounds have enjoyed widespread application in photochemistry [1,2], organic optoelectronics [3,4], and luminescent sensors [5,6]. In contrast to conventional organic fluorophores, which are singlet emitters, transition metal complexes display triplet emission due to spin–orbit coupling imparted by the heavy atom effect, which leads to efficient singlet–triplet state mixing and enhancement of phosphorescence quantum efficiency. The phosphorescence behavior of metal complexes has found potential for the construction of organic light-emitting diodes (OLEDs) for display or lighting applications [7–10].

In the context of luminescent sensing, transition metal complexes have unique advantages that make them suitable for chemosensing or biosensing applications. These include their (i) high luminescence quantum yield, (ii) long phosphorescence lifetime that allows their emission to be distinguished from a fluorescent background, (iii) large Stokes shift for effective discrimination of excitation and emission wavelengths, (iv) sensitivity of their emissive properties to subtle changes in the local environment, and (v) modular synthesis that allows facile synthesis of analogues for fine-tuning of their chemical and/or photophysical properties.

In light of these advantages, transition metal compounds have been widely studied for luminescent sensing applications, particularly the d^6, d^8 or d^{10} electron complexes based on ruthenium(II), platinum(II), iridium(III), osmium(II), gold(I), zinc (II) and rhenium(I). Compared with organic fluorophores, the excited state properties of transition metal complexes are complicated and can include metal-to-ligand charge-transfer (MLCT), ligand-to-ligand chargetransfer (LLCT),

intraligand charge-transfer (ILCT), ligand-to-metal charge transfer (LMCT), metal–metal-to-ligand charge-transfer (MMLCT), ligand-to-metal–metal charge transfer (LMMCT) and metal-to-ligand–ligand charge-transfer (MLLCT) states [11,12]. The properties of the excited states are highly sensitive to the metal centre, the type of ligands, and the nature of the local environments, allowing the photophysical properties (such as emission wavelength, lifetime, and intensity) of metal complexes to be tailored for specific applications.

A chemosensor is a compound that renders a significant change in electrical, electronic, magnetic, or optical signal when it binds to a specific guest counterpart. In the past decades chemosensors have been widely investigated for their fundamental role in medical, environmental and biological applications [18]. A great many efforts have been made for designing and synthesizing sensors with high selectivity, sensitivity, low detection limit and instantaneous response [19]. Of those sensors, fluorescent chemosensors have several advantages over others due to their sensitivity, specificity, and real-time monitoring with fast response time [20]. In this connection, considerable efforts have been made to synthesize fluorescent chemosensors that are selective, sensitive, and suited to highly resolved imaging for monitoring biological processes [24].

It is highly demanding to selectively sense heavy metal ions such as mercury, lead, and copper. Copper plays an important role in various biological processes [21], it is indispensable in its interactions with certain proteins to produce numerous metalloenzymes such as superoxide dismutase, cytochrome c oxidase and tyrosinase that are critical for life. However, copper is toxic when its concentration exceeds cellular needs and has been linked to neurodegenerative diseases such as Alzheimer's disease and Wilson's disease [23].

Recently, many fluorescent chemosensors for Cu(II)-selective detection were reported and have been used with some success in biological applications [25]. However, some of them have shortcomings for practical application such as

sensitivities toward other metal cations, low water solubility, a narrow pH span, slow response, a low fluorescence quantum yield in aqueous media, and cytotoxicities of ligand. Despite that a number of fluorescent chemosensors have been reported, the studies regarding detailed sensing mechanisms are scarce.

The biopolymer DNA is the primary carrier of all genetic information. The central dogma of molecular biology underlines its central role in the storage and replication of genes. Through the RNA mediated processes of transcription and translation, DNA provides the ‘‘master genetic blueprint’’ for the synthesis of each protein required by individual cells. All these processes are initiated, regulated, and terminated by small molecules and/or proteins that bind to nucleic acids in site-specific ways. Consequently, synthetic molecules that interact with nucleic acids or modulate their function have found a variety of uses as biophysical and therapeutic agents [26].

In many ways, coordination complexes are ideal templates for the design of DNA-interactive systems, and the interaction of these structurally complex three-dimensional architectures with DNA is becoming increasingly studied. In addition to a variety of binding modes, metal complexes also offer distinctive chemical activities: they can coordinate directly to DNA Lewis base sites; they can undergo redox reactions with DNA or generate reactive oxygen containing species (an attribute particularly relevant to photodynamic therapy, PDT). The ability to bind to and cleave DNA, and thus interfere with the essential cellular processes of transcription and translation, means that these systems could also be developed as potential therapeutics. Last, but certainly not least, metal complexes often display photophysical properties that can be exploited in the construction of diagnostic and imaging probes.

In the last few years, cellular studies involving a spectrum of luminescent metal complexes have become increasingly common. This work has centred on the biological application of such systems, particularly focusing on achieving DNA targeting. Nucleic acids are the most fundamental and important class of biomolecules

in a living cell. Their detection and characterization are therefore of great importance, which would not only help us to understand how the cell functions and to assist biological research, but also facilitate the development of new tools for disease diagnosis and treatment and developments of new drug.

Yam *et al.* demonstrated a general label-free method for optical sensing and characterization of single-stranded nucleic acid [27]. The electrostatic binding of positively charged Pt(II) complex [28] to single-stranded nucleic acids carrying multiple negative charges can induce the aggregation and self-assembly of planar Pt(II) complexes, leading to remarkable changes in optical properties.Furthermore, they realized the detection of DNA G-quadruplex formation and nuclease activity through aggregation-induced spectral changes of Pt(II) complex [29]. Phenanthridine derivatives, such as ethidium bromide and propidium iodide, are a kind of widely used probe for detecting the presence of duplex nucleic acids [30]. Turro *et al.* introduced a phenanthridine moiety to Ru(II) complex and found that this complex can act as a RNA probe with a nine-fold enhancement in signal intensity and a fluorescence lifetime many times greater than that of other phenanthridine derivatives in the presence of RNA, making it especially useful for timer esolved detection in complex biological solutions such as cell growth medium [31].

In this connection, considerable efforts have been made to synthesize transition metal complexes as fluorescent biosensors that are selective & sensitive DNA binders and suited to highly resolved imaging for monitoring biological processes. Recently, ruthenium and platinum complexes for DNA detection were reported and have been used with some success in biological applications [32]. However, some of them have shortcomings for practical application such as low water solubility, a narrow pH span, and cytotoxicity of ligand.

Thus developing cheap and practical chemosensors for Cu^{2+} and DNA remains a great challenge. Herein we report, the synthesis and spectroscopic characterization of six mixed ligand dipeptide complexes of VO^{2+} and Zn2+ with moxifloxacin (MFL). The

vanadyl complexes were found to be a highly selective probes for Cu^{2+} and could be used to detect Cu^{2+}.wheras zinc complexes could bind strongly to DNA and act as sensors for DNA.

8.2 General synthesis of complexes

8.2.1 Synthesis of Vanadyl (II) complexes

To a stirred methanolic solution (10 ml) of oxovanadium(IV) sulfate (0.25 g, 1.0 mmol) was added an aqueous solution the dipeptide (1.0 mmol) [glycyleucine, glycylglycine and glycylalanine] followed by drop wise addition of KOH (0.056 g, 1.o mmol) . The reaction mixture was stirred for 2 h at room temperature to obtain a clear green color solution. A methanolic solution (20 ml) of moxifloxacin (MFL) (0.401 g, 1.0 mmol) was added to the above reaction mixture and refluxed for another 2 h. The green colored solid was filtered, thoroughly washed with ice cold methanol and dried in vacum over anhydrous $CaCl_2$. The reaction for the synthesis of the complexes has been given in Scheme 1. The complexes were characterized by IR, ESR, Mass spectral and elemental analysis techniques.

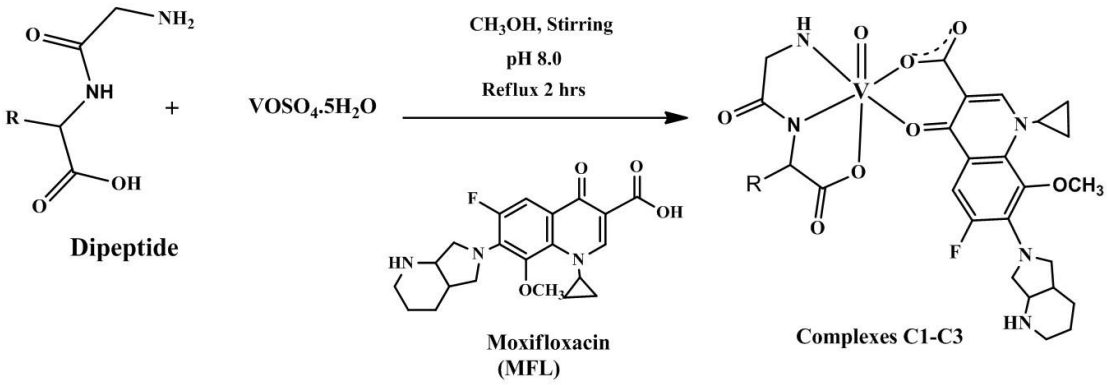

-R	dipeptide	Complex
$CH_2CH(CH_3)_2$	glycyleucine	C1
-H	glycylglycine	C2
$-CH_3$	glycylalanine	C3

Scheme 8.1.

8.2.2 General synthesis of Zinc complexes

To a stirred methanolic solution (10 ml) of Zinc(II) nitrate (1.0 mmol) was added an aqueous solution the dipeptides (1.0 mmol) [glycyleucine, glycylglycine and glycylalanine] followed by drop wise addition of KOH (1.0 mmol) . This reaction mixture was stirred for 30 min at room temperature to obtain clear solution. A methanolic solution (20 ml) of moxifloxacin (MFL) (1.0 mmol) was added to the above reaction mixture and refluxed for another 2 h. The white colored solid was filtered, thoroughly washed with ice cold methanol and dried in vacum over anhydrous $CaCl_2$. The reaction scheme for the synthesis of the complexes has been given in scheme 8.2.

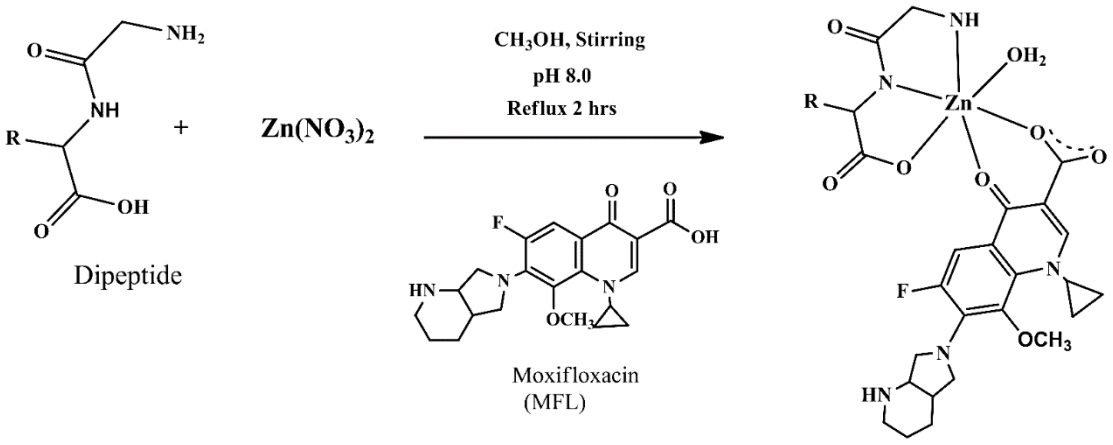

-R	dipeptide	Complex
$CH_2CH(CH_3)_2$	glycyleucine	C4
-H	glycylglycine	C5
$-CH_3$	glycylalanine	C6

Scheme 8.2

8.3 Physicochemical data of Complexes

A. [VO(glyleu)(MFL)] **(C1)**

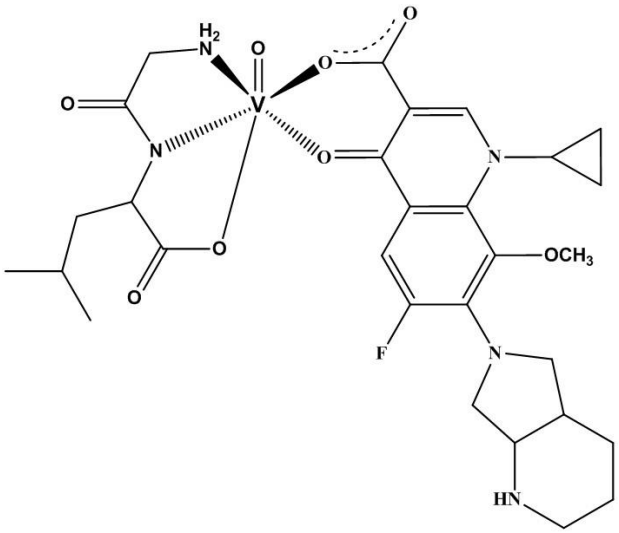

Yield: 75 %
Molecular weight: 655.59 g/mol
Molecular formula: $C_{29}H_{38}FN_5O_8V$
Calc. (%): C, 53.21; H, 5.85; N, 10.70.; V, 7.78.
Found (%): C, 54.21; H, 5.85; N, 10.60.; V, 7.8
λ_{max}: 224, 288, 333 nm.
ESI-MS [MeOH, *m/z*]: 656.2[M+1]

B. [VO(glygly)(MFL)] **(C2)**

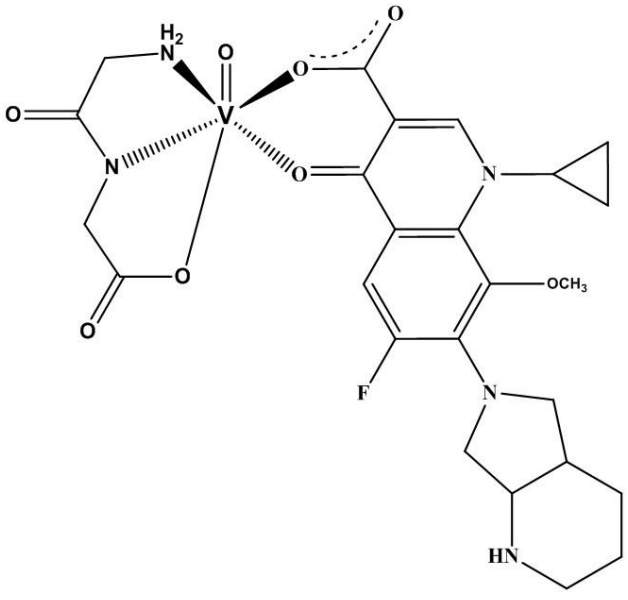

Yield: 78 %
Molecular weight: 598.45g/mol
Molecular formula: $C_{25}H_{30}FN_5O_8V$
Calc. (%): C, 50.17; H, 5.05; N, 11.70.; V, 8.51
Found (%): C, 51.0; H, 5.10; N, 11.60.; V, 8.5
λ_{max}: 231, 293, 342 nm.
ESI-MS [MeOH, *m/z*]: 599.2[M+1]

C. [VO(glyala)(MFL)] **(C3)**

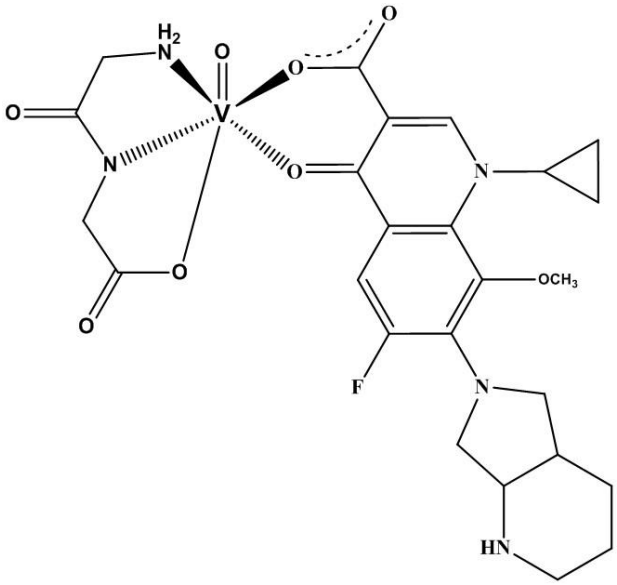	Yield: 71 % Molecular weight: 612.50 g/mol Molecular formula: $C_{26}H_{32}FN_5O_8V$ Calc (%): C, 50.98; H, 5.27; N, 11.43.; V, 8.32. Found (%): C, 51.0; H, 5.26; N, 11.50.; V, 8.30 λ_{max}: 231, 293, 344 nm. ESI-MS [MeOH, *m/z*]: 612.0[M^+]

D. [Zn(glyleu)(MFL)(H_2O)] **(C4)**

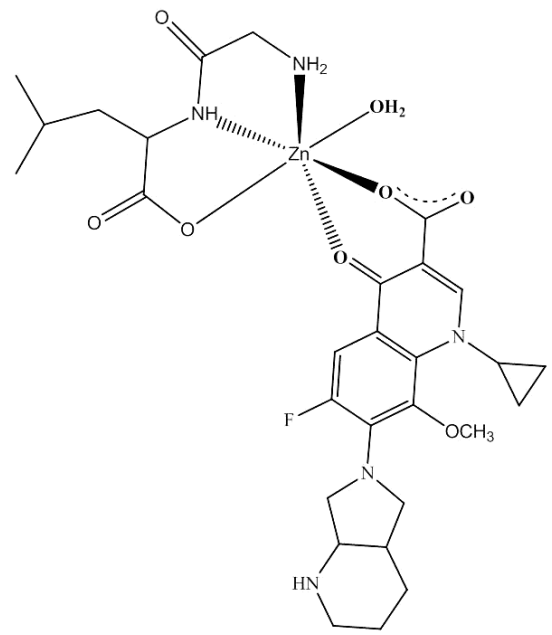	Yield: 81 % Molecular weight: 687.08 g/mol Molecular formula: $C_{30}H_{44}FN_5O_8Zn$ Calc. (%): C, 52.44; H, 6.45; N, 10.19.; Zn,9.52. Found (%): C, 53.00; H, 6.59; N, 10.28.; Zn, 9.64 λ_{max}: 290,224, 336nm. ESI-MS [MeOH, *m/z*]: 685.2 [M-1]

E. [Zn(glygly)(MFL)(H_2O)] **(C5)**

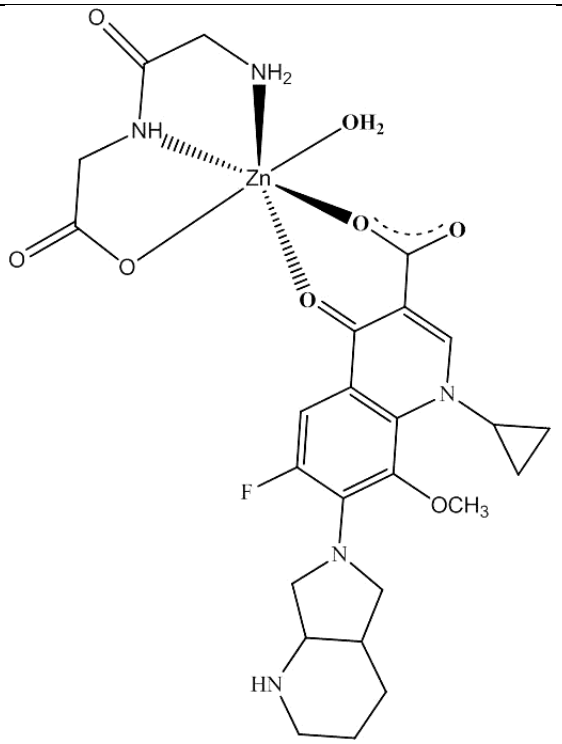	Yield: 86 % Molecular weight: 630.97g/mol Molecular formula: $C_{26}H_{36}FN_5O_8Zn$ Calc. (%): C, 49.49; H, 5.75; N, 11.10.; Zn, 10.36 Found (%): C, 50.0; H, 5.68; N, 11.00.; Zn,10.35 λ_{max}: 293,293, 338 nm. ESI-MS [MeOH, *m/z*]: 629.2[M-1]

E. [Zn(glyala)(MFL)(H_2O)] **(C6)**

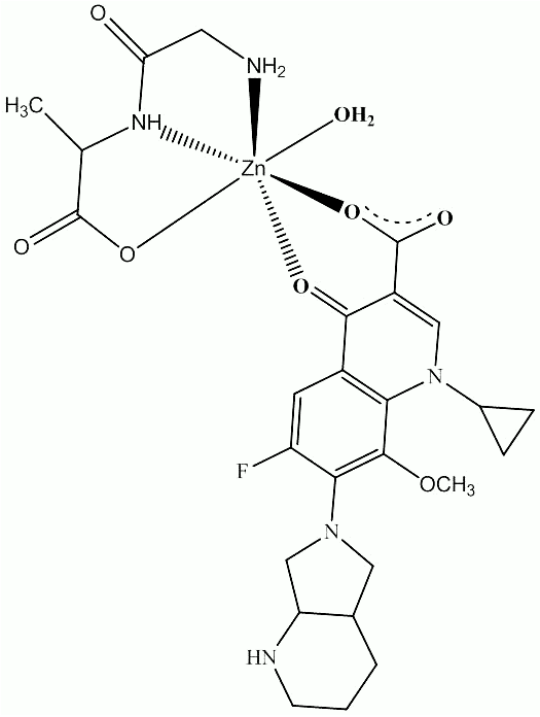	Yield: 79 % Molecular weight: 643.20 g/mol Molecular formula: $C_{27}H_{38}FN_5O_8Zn$ Calc (%): C, 50.28; H, 5.94; N, 11.43.; Zn, 10.14 Found (%): C, 51.0; H, 5.26; N, 11.50.; Zn, 10.25 λ_{max}: 291, 228, 339 nm. ESI-MS [MeOH, *m/z*]: 643.0[M^+]

8.4 Results and discussions

8.4.1 Synthesis and general properties

Mixed ligand VO(II) complexes [VO(glyleu)(MFL)](C1), [VO(glygly) (MFL)] (C2) and [VO(glyala)(MFL)] (C3) were obtained from methanol solution, by reaction of Vanadyl sulphate with dipeptides and MFL in 1:1:1 molar ratio (scheme 8.1). The isolated compounds were then characterized by physico chemical and analytical methods.

The synthesis of Zn(II) complexes (C4-C6) was achieved by mixing stoichiometric amounts of Zn(II) nitrate hexahydrate with dipeptides (glycleucine, glycylglycine and glycylalanine) and MFL (scheme 8.2), in a good yield. The composition of the complexes was ascertained by elemental analysis, IR, UV–vis, ESI–MS spectroscopy.

The ESI-MS spectra of complexes C1-C6 showed molecular ion peaks at m/z 656 .0[M+1], 599.0 [M+1], 612.0 [M^+], 685.2 [M-1], 629.2 [M-1] and 643.0 [M^+] respectively with the experimental molecular weight values matching the calculated values, confirming thereby the composition of the complexes (Fig.8.1(a)and(b)). Furthermore the composition and purity of the complexes have been confirmed by their C, H, N elemental analysis.

The FTIR spectra of C1-C6 were recorded in the region 4000–400 cm^{-1} (Fig. 8.2) and analyzed in comparison to the spectra of the free ligands. In the IR spectra, the absorption bands at 1374-1385cm^{-1} are characteristic C-N stretch of the deprotonated peptide nitrogen bound to the metal ion. The N-H bending vibration (amide II band) observed at 1575cm^{-1} in the free dipeptides has disappeared in the complexes due to deprotonation and coordination of the peptide nitrogen. The $\nu(CO)_{peptide}$ band (amide I) is shifted to 1608-1623cm^{-1} due to the involvement of the depronated peptide nitrogen in bonding with vanadyl and Zinc ion, which lowers the bond order of the ν(CO)amide group due to resonance stabilization and further confirmed the coordination of metal ions through peptide-N atom [32]. The shift in the bands

corresponding to $\nu_{asym}(COO)_{pep}$ and $\nu_{sym}(COO)_{pep}$ suggested the involvement of the carboxylic group of the dipeptides in complex formation. A broad band at 3317-3242 cm^{-1} observed in the IR spectra of complexes is attributed to N-H stretch of the terminal amino group of the dipeptides which was shifted to lower frequency upon coordination [33]. Similarly the shifts in the pyridone carbonyl $\nu(CO)_{MFL}$ and carboxylate $\nu(COO)_{MFL}$ stretching frequencies of moxifloxacin in complexes indicated the binding of these groups with the metal ions. The IR data have been presented in table 8.1.

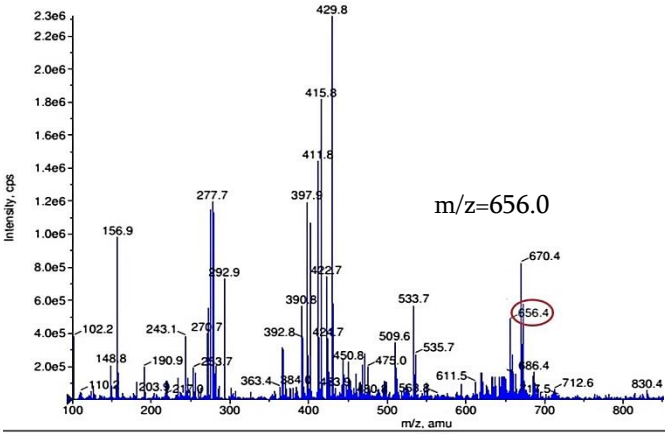

Fig 8.1 (a): ESI-MS spectra of **C1**

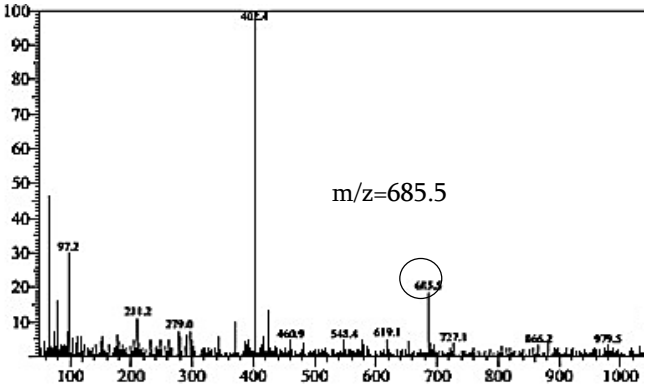

Fig 8.1 (b): ESI-MS spectra of **C4**

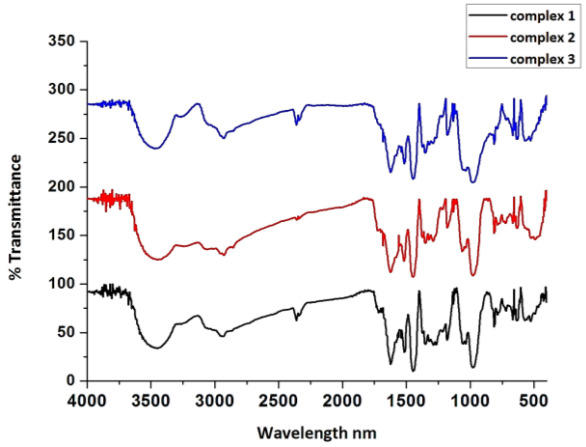

Fig 8.2: IR spectra of **C1-C3** in the range of 4000-400 cm^{-1}

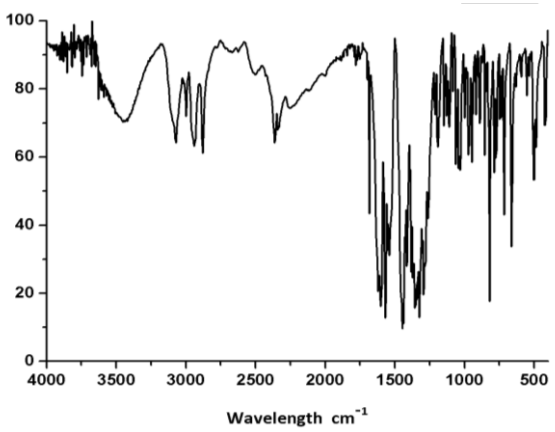

Fig 8.2(b): IR spectra of **C4** in the range of 4000-400 cm^{-1}

Table 8.1: Characteristic IR bands (4000–400 cm^{-1}) of **C1-C6**.

Complexes	δ(NH)+ν(C–N) amide II and III bands cm^{-1}	ν(CO) peptide [amide I] cm^{-1}	ν $(COO)_{asym}$ and ν $(COO)_{sym}$ peptide cm^{-1}	$(N-H)_{pep}$ cm^{-1}	ν $(COO)_{asym}$ and ν $(COO)_{sym}$ cm^{-1}	$\nu(CO)_{py}$ MFL cm^{-1}	V=O cm^{-1}	Zn-O & Zn-N cm^{-1}
Dipeptides	1575 and 1254	~1665	1586 &1410	3317	-	-	-	
MFL	-	-	-		1625	1720	-	
C1	1374	1623	1515 &1445	3230	1513 & 1354	1683	975	
C2	1379	1623	1518 & 1445	3223	1518 & 1353	1683	976	
C3	1375	1623	1515 & 1445	3242	1513 & 1355	1683	976	
C4	1385	1612	1556 & 1440	3218	1518 & 1350	1679	-	424 & 463
C5	1381	1608	1551 & 1441	3221	1517 & 1352	1675	-	425 & 460
C6	1379	1609	1549 & 1440	3221	1514 & 1350	1678	-	424 & 460

The electronic absorption spectra of **C1-C6** in freshly prepared dmso solutions was observed in the region 200–900 nm at room temperature (Fig. 8.3 (a) and (b)). The electronic spectra of free dipeptides displayed intense absorption bands at 220 nm due n-π* transition, which shifted to 224-231 nm in the spectra of complexes[34] . Broad bands at 288-293 and 333-344 nm for **C1-C6** were attributed to π→π* and n→π* transitions of moxifloxacinato ligand [35]. In the visible region, low-intensity bands at ~851-861nm assigned to a b_2 (dxy) → e_π^*(dxz; dyz) transitions of the VO^{2+} ion are observed in the complexes **C1-C3**. Intense bands observed at 398-406 nm are attributed to stronger moxifloxacin ligand-to-metal charge-transfer transitions for **C1-C3.** These bands are typical for distorted octahedral VO^{2+} complexes.

Table 8.2: Characteristic bands λ_{max} (nm) in the UV–Vis spectra of **C1-C6**.

Ligands	Intraligand band $\pi \rightarrow \pi^*$ (nm)	Intraligand band $n \rightarrow \pi^*$ (nm)	LMCT MFL $\rightarrow VO^{2+}$ (nm)	d-d transition (nm)
Dipeptides	-	220	-	-
MFL	290	337	-	-
Complexes				
C1	288	224, 333	406	861
C2	293	231, 342	398	858
C3	293	231, 344	399	851
C4	290	224, 336	-	-
C5	293	228, 338	-	-
C6	291	228, 339	-	-

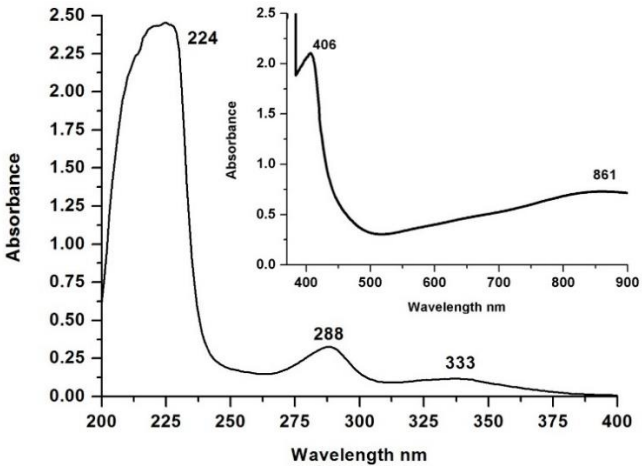

Fig 8.3: Electronic spectra of **C1** in dmso. Inset shows the visible spectra of the complex **C1**.

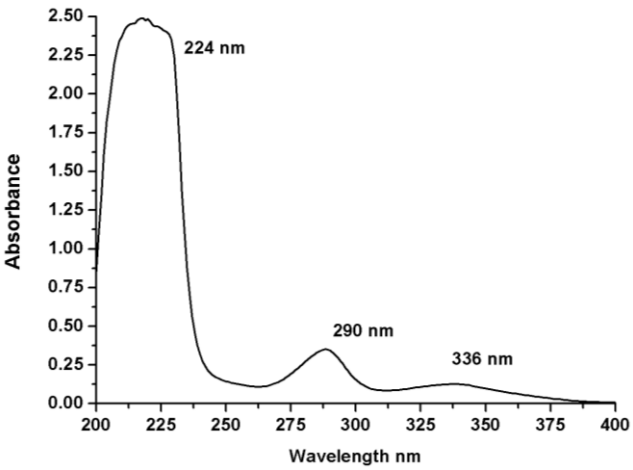

Fig 8.3 (b): Electronic spectra of **C4** in dmso.

The X-band EPR spectra of **C1-C3** were recorded in frozen DMSO solution at 110 K. The spectra exhibites the expected hyperfine eight-line pattern, characteristic of an unpaired electron being coupled with a vanadium nuclear spin (I=7/2) (Fig. 8.4). The $g_{//} >> g_{\perp}$ and $A_{//} >> A_{\perp}$ relationships (Table 8.3) are characteristic of an axially compressed d_{xy}^1 configuration [36]. On the basis of the additivity relationship, the experimental $A_{//}$ values were found to be close to the calculated $A_{//}$ value for the oxovanadium complexes [37, 38] . Thus, the most reasonable equatorial donor atom set is N_2O_2 ($O_{carboxylate}$, $O_{pyridone}$, N_{imine} and N_{amine}) for the oxovanadium complexes in DMSO solution. The EPR hyperfine profile is similar to those of many other oxovanadium(IV) complexes reported earlier [39].

Table 8.3: X-band ESR parameters of **C1-C3**.

Compounds	$g_{\parallel}$	$g_{\perp}$	G	$A_{\parallel}$	$A_{\perp}$
C1	2.04	2.002	6.3	$164x10^{-4}$	$35.3x10^{-4}$
C2	2.07	2.008	6.1	$167x10^{-4}$	$33.3x10^{-4}$
C3	2.03	2.006	5.5	$165x10^{-4}$	$36.2x10^{-4}$

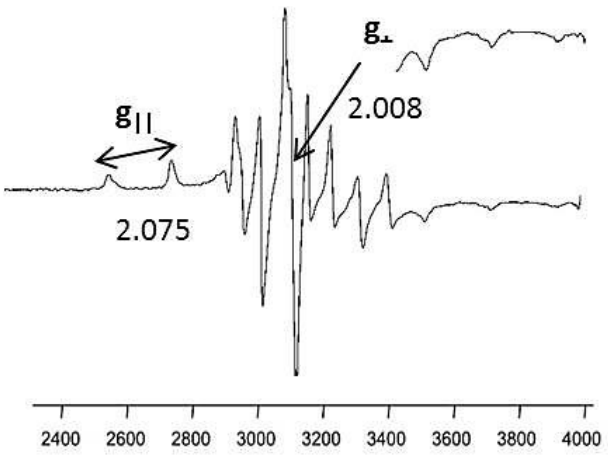

Fig 8.4: ESR Spectra of **C1** in DMSO.
EPR conditions: Temperature, 10K; microwave power, 5.0 mW;
Modulation amplitude, 1G; microwave frequency, 9.1GHz.

The thermal stability of complexes **C1**-**C3** were examined using TG and DTA analysis. The TG curves (Fig.8.5(a)) show two-decomposition steps, (a) loss in weight corresponding to loss of dipeptide ligands in the range of 100–420 °C and (b) weight loss between 440–800 °C due to loss of MFL ligand leading to V_2O_5 as a residue

The thermal stability of complexes **C4**-**C6** were examined using TG and DTA analysis (Fig. 8.5(b)).The TG curves show two-decomposition steps, (a) loss in weight corresponding to loss of coordinated water and dipeptide ligands in the range of 100–320 °C and (b) weight loss between 320–800 °C due to loss of MFL ligand leading to ZnO as a residue.

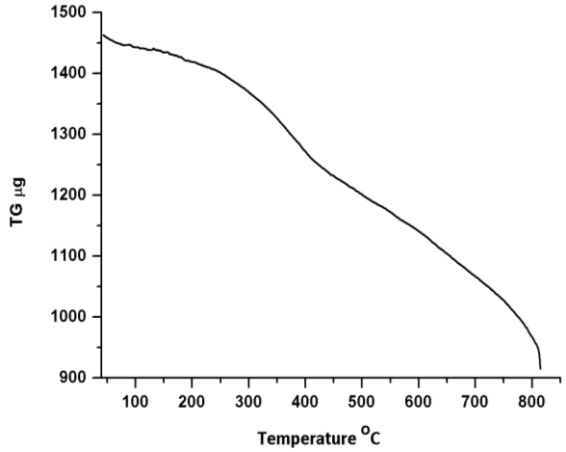

Fig 8.5(a): Thermal degradation curve of **C1** at heating rate of 10 °C per minute under N_2 atmosphere

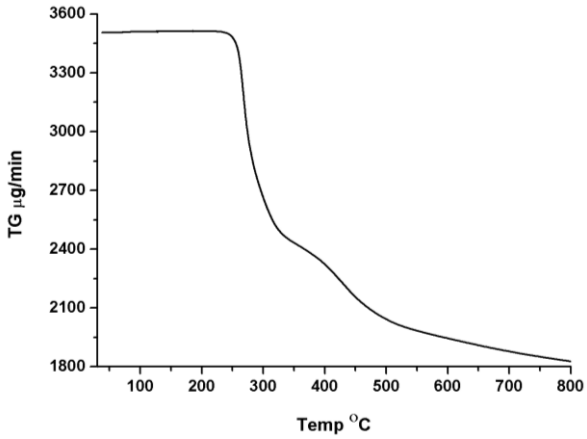

Fig 8.5 (b): Thermal degradation curve of **C4** at heating rate of 10 °C per minute under N_2 atmosphere

8.4.2 VO (II) complexes as sensors for Cu^{2+}

8.4.2.1 UV-Visible titrations

The absorption spectrum of the **C1** (20 μM) in dmso solution exhibited bands at 288nm and 340nm assigned to a π-π* and n-π* transitions of the moxifloxacinato ligands, respectively. To investigate the cation response of **C1**, thirty equivalence (600 μM) of the metal salts (Cu^{2+}, Ni^{2+}, Co^{2+}, Zn^{2+}, Na^{+}, K^{+}, Cd^{2+}, Al^{3+}) were added to the solution of **C1** and the spectrum was recorded in the presence of the metal ions. The addition of metal ions other than Cu^{2+} induced a slight red shift (~4 nm) of the π-π* band and slight increase in absorption intensity (Fig. 8.6(a)). A red shift in the peak at 340 nm was also observed upon addition of Ni^{2+} with negligible increase in absorption. In contrast the addition of Cu^{2+} lead to a remarkable increase in absorption intensity along with similar shifts in the absorption peaks.

To further establish the Cu^{2+} response of **C1**, UV-titration of solution of **C1** (20 μM) with increasing concentration (0-600 μM) of Cu^{2+} was performed. A steady increase in the absorption intensity of the peak at 288nm (Fig. 8.6(b)) was observed. UV-titration of complexes **C2** and **C3** with increasing concentrations of Cu^{2+} also showed an increase in the absorption intensity of the peak at 293nm (π-π*)indicating the selective sensing capability of the complexes **C1-C3** for Cu^{2+}.

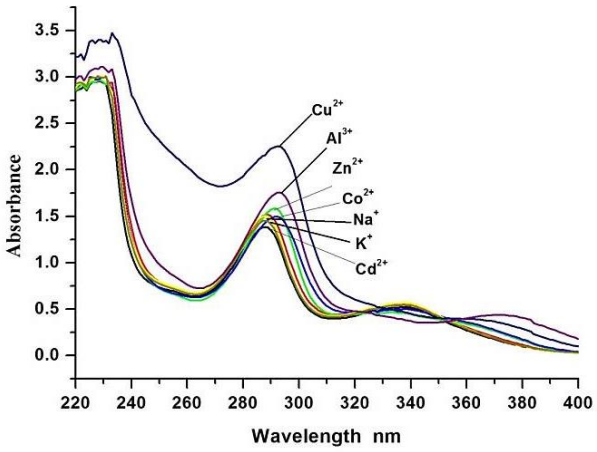

Fig 8.6 (a): Absorption spectra of **C1** (20 μM) in water-dmso (v/v = 9:1), in presence of different metal cations (30 equiv.)

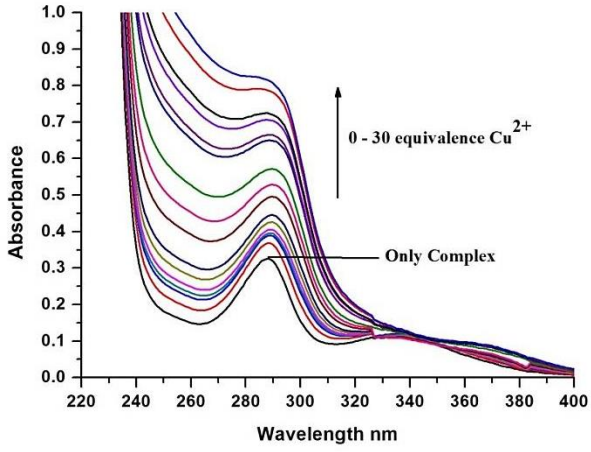

Fig 8.6 (b): Absorption spectra of **C1** (20 μM) in water-dmso (v/v = 9:1), in presence of 0-30 equivalence of Cu^{2+} (0-600 μM).

8.4.2.2 Fluorescence measurements

Fluorescence titrations of **C1** with different metal cations were carried out and the results are shown in Fig. 8.7. The excitation of the absorption band at λ_{max}=288 nm caused emissions at 470nm for **C1.** The addition of Mg^{2+}or Pb^{2+} induced negligible change in the emission intensity of **C1**, whereas other cations such as Zn^{2+},Cd^{2+},K^{+},Na^{+}, Cr^{3+} and Co^{2+} triggered slight emission quenching. In contrast, Cu^{2+} caused complete quenching of fluorescence (Fig. 8.7(a)).

A detailed spectrofluorimetric titration was performed by adding 0-600μM of Cu^{2+} to solutions of **C1**(20 μM) in Tris-HCl buffer at 25±1^{0}C .Upon addition of increasing amounts of Cu^{2+}, a rapid decrease in the intensity of the emission band was observed (Fig. 8.7(b)). Similar results were obtained for **C2** & **C3**.

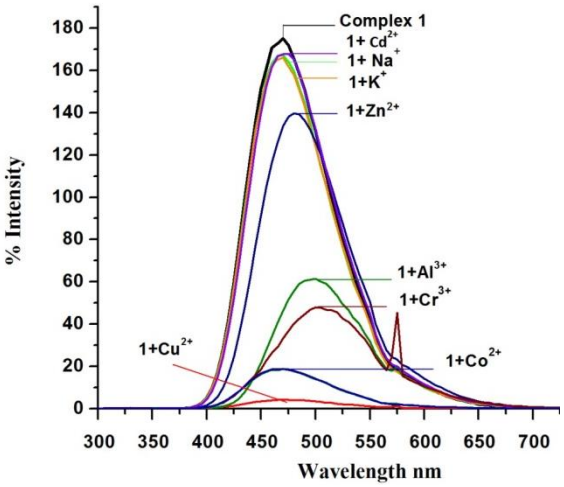

Fig 8.7(a): Emission spectra of **C1** (20 μM) upon addition of 30 equiv of different metal ions in water-dmso (v/v = 9:1) solutions when excited at 288 nm.

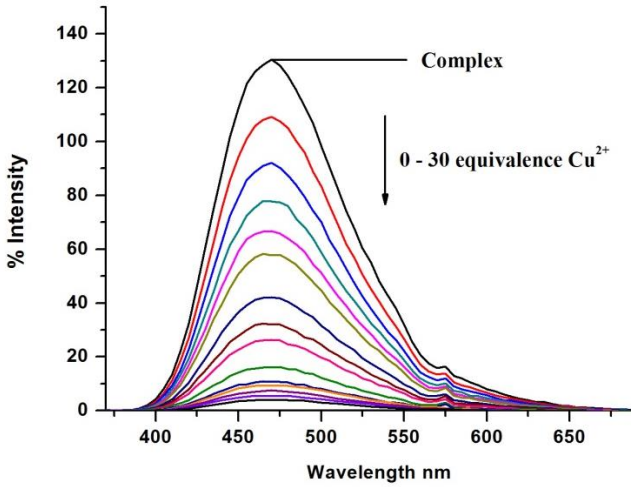

Fig 8.7(b): Emission spectra of **C1** (20 μM) with various amounts of Cu^{2+} (0-600μM) in water-dmso (v/v = 9:1) solutions (λ_{ex}= 288 nm).

Complete quenching of fluorescence was observed when Cu^{2+} (600 μM) was added to a solution of **C1** (20 μM) as shown in Fig. 8.8(a). No such quenching was observed on the addition of other metal ions. A gradual decrease in fluorescence intensity was also observed on addition of increasing amounts of Cu^{2+} (0-600 μM) to a solution of **C1** as shown in Fig. 8.8(b) .

Fig 8.8: (a) Photograph of **C1** (20 μM) solutions containing different metal ions (600 μM).

Fig 8.8: (b) Photograph of **C1** (20 μM) solutions containing Cu^{2+}(0-30 equivalence)

8.4.2.3 Evidence for replacement of VO^{2+} by Cu^{2+}

To get deep insight into the changes taking place after addition of Cu^{2+} that results in the quenching of fluorescence of complexes, electrospray ionization (ESI) mass spectra of complexes **C1-C3** in the presence of Cu^{2+} were obtained. The mass spectra exhibited m/z peaks corresponding to the mixes ligand [Cu(dipep)(MFL)] complexes (Fig. 8.9 (a)) indicating complete replacement of VO^{2+} and complexation by Cu^{2+} (Fig. 8.9 (b), Table 8.4).

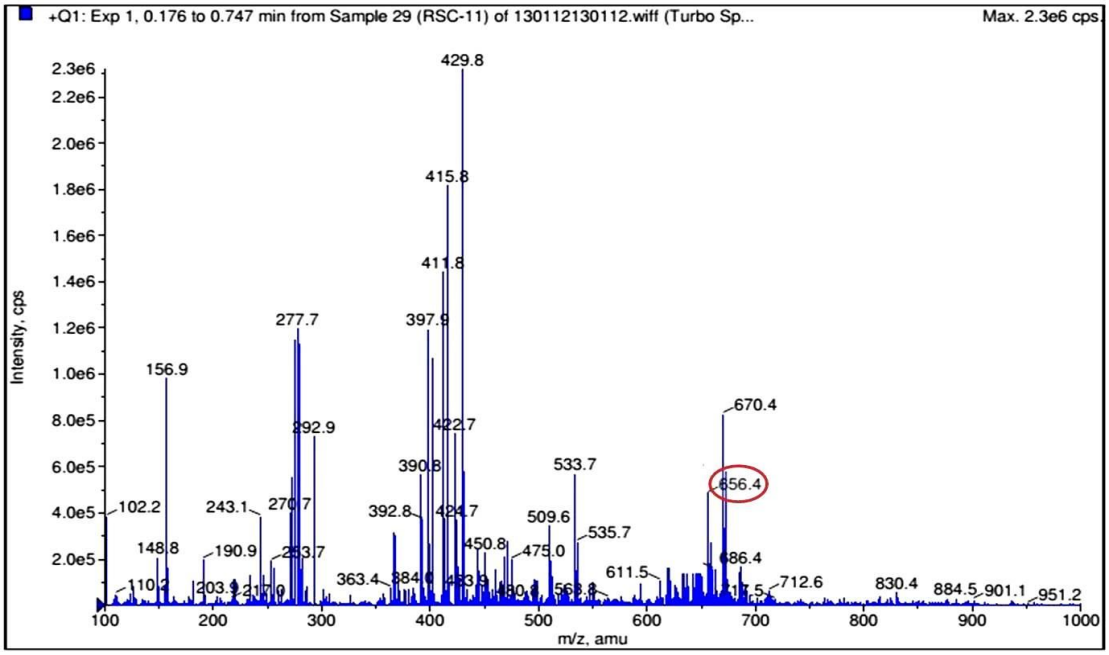

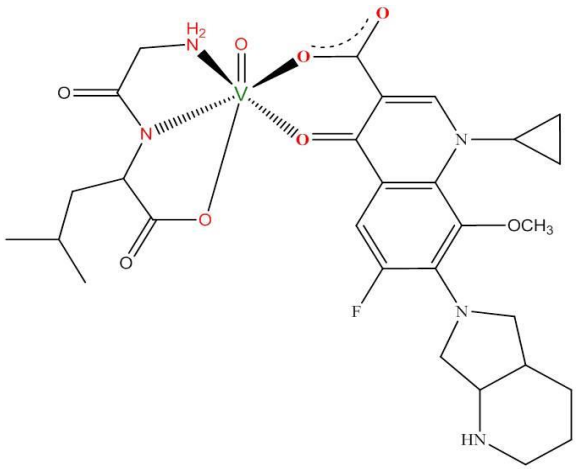

Chemical Formula:
$C_{29}H_{38}VFN_5O_8$
Exact Mass: 655.59

Fig 8.9(a): Mass spectra of **C1**

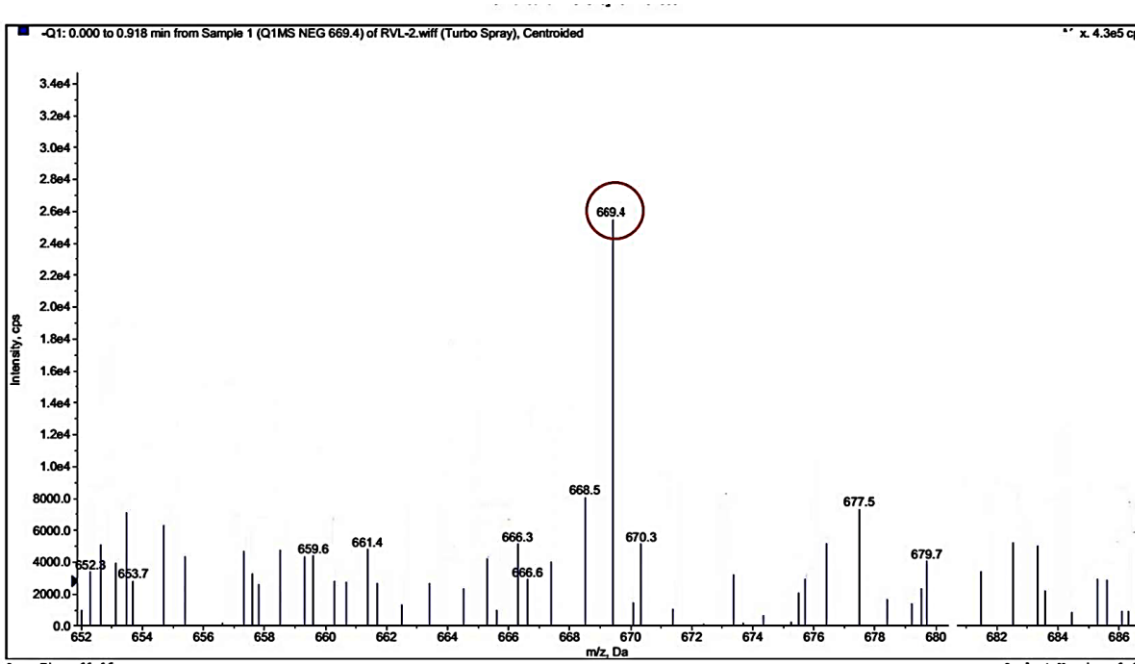

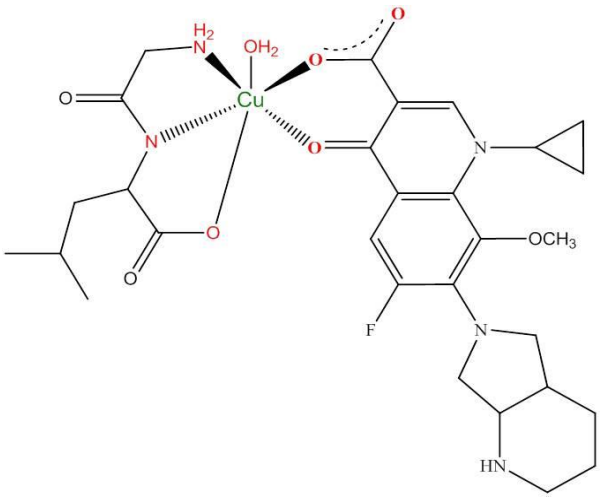

Chemical Formula: $C_{29}H_{40}CuFN_5O_8$
Exact Mass: 669.20

Fig 8.9(b): Change in mass spectra of **C1** after addition of Copper (II).

Table 8.4: Change in the mass spectra of **C1-C3** after addition of Cu^{2+}.

Compounds	m/z	Change in m/z after addition of Cu^{2+}
C1	656.4	669.20
C2	598.8	613.17
C3	612.4	626.17

Replacement of the VO^{2+} by Cu^{2+} and formation of [Cu(glygly)(MFL)(H_2O)] complexes was also confirmed by the absence of V=O peak in the FTIR spectra of **C1** in the presence of Cu^{2+} (Fig. 8.10).Similar results were obtained for complex **C2** and **C3**.

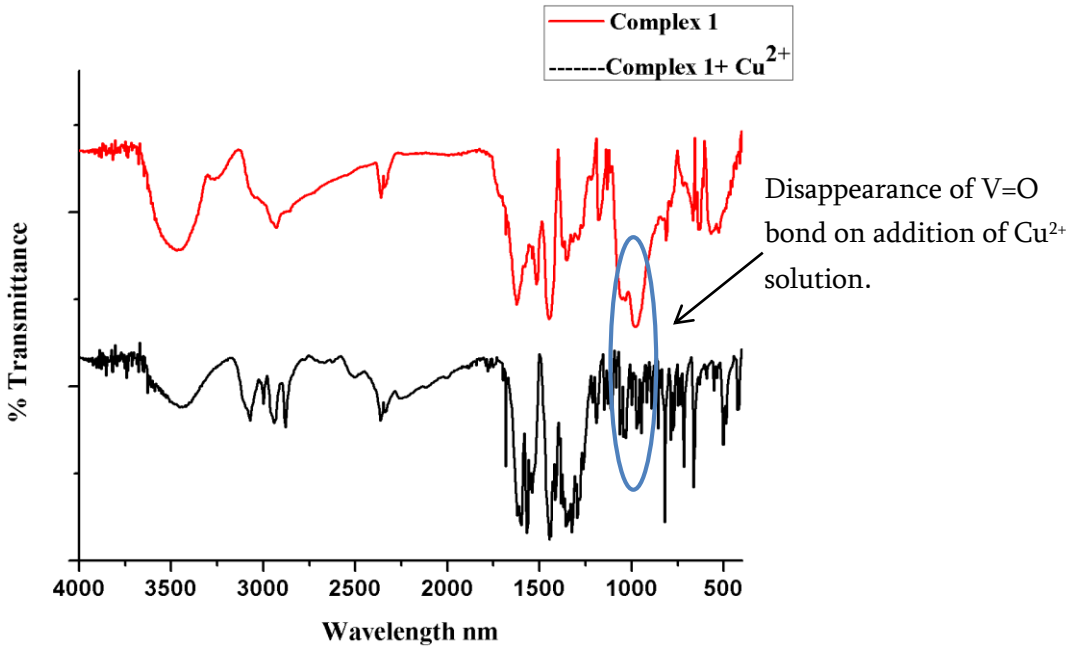

Fig 8.10: IR spectral changes of **C1** on addition of Cu^{2+} solution.

The quenching of fluorescence upon complexation with Cu^{2+} originate partly due to interactions between the excited MFL ligand and the non-excited Cu^{2+}.The electronic excited energy may be transferred from MFL π molecular orbital to the Cu^{2+} dπ molecular orbital by energy transfer and electron transfer process. The Cu^{2+} ion is formally reduced and the ligand MFL is formally oxidised. The π electron in the higher energy orbital of the ligand is transferred to an electron deficient Cu^{2+} ion quencher. The hole left due to promotion of an electron, accept an electron from the electron rich quencher. Other than electron transfer process, energy transfer process can also cause quenching of fluorescence [40]. Energy is transferred from the excited state of the complexes **C1-C3** to the non-excited Cu^{2+} ion on complexation, by non-radiative decay thus quenching fluorescence. The results impllied that **C1** could act as a chemosensor for selective detection of Cu^{2+} and can replace the V(IV) in **C1**. Similar results were observed for complexes **C2** and **C3**.

8.4.3 Zn(II) complexes as sensors for DNA.

8.4.3.1 UV-vis absorption titrations

The DNA binding studies of **C4-C6** with CT DNA were carried out by employing electronic absorption spectroscopy. All the complexes exhibited intense absorption bands at ~290 nm and a broad band at ~336 nm attributed to $\pi \rightarrow \pi^*$ and $n \rightarrow \pi^*$ intraligand transition, respectively. The spectral changes in the absorption spectra of the complexes in the absence and in presence of CT-DNA are shown in the Fig.8.11(a). Addition of increasing concentration of CT-DNA (0-200x10^{-6} M) to a fixed concentration of **C4-C6** (6.60 x 10^{-6} M) resulted in a pronounced "hyperchromism" of 72%, 69% and 70% respectively, with small red shift of the intraligand absorption band. These spectral characteristics are speculative of groove binding nature of complexes. The intrinsic binding constant value K_b for complexes **C4–C6** were 7.8 x10^6, 5.2 x10^6 , and 6.9 x10^6 M^{-1} respectively (Fig. 8.11(b)).

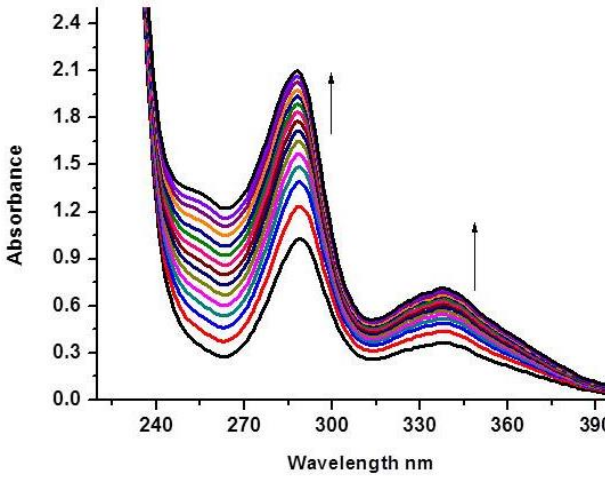

Fig 8.11(a): Absorption spectraof **C4** showing the increase in absorption intensity on gradual addition of CT-DNA in 5 mM TrisHCl buffer (pH,7.2) at 25°C.

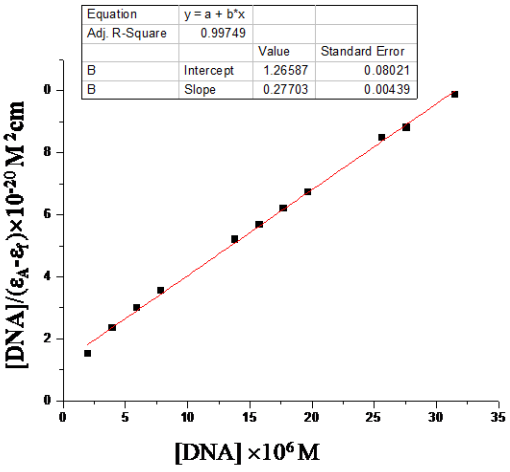

Fig 8.11(b): Plot of [DNA]/(ε_A-ε_f) vs [DNA] for the titration of **C4** with CT-DNA.

8.4.3.2 Emission spectral studies

To examine the mode of binding of the compounds with DNA, a competitive binding studies with two dyes: EB and DAPI were been carried out using steady state fluorescence spectroscopy. The emission intensity of EB was used as a spectral probe. EB shows reduced emission intensity in buffer solution because of solvent quenching and an enhancement of the emission intensity when intercalated to DNA. The emission spectra of DNA–EB (λ_{ex}= 546 nm, λ_{em}= 610) in the absence and presence of increasing amounts **C4-C6** have been recorded. Addition complexes **C4–C6** did not have any kind of effect on the emission intensity or nature of the emission of DNA–EB complex. This indicated that the complexes could not replace EB from DNA-EB complex, which further confirmed their non-intercalative binding mode which was also evident from UV-Vis absorption titration.

To further confirm the groove binding of the complexes competitive binding studies with DAPI (a classical minor groove binder to DNA) was carried out. The fluorescence spectra of a mixture of DNA–DAPI solution with increasing concentration of **C4** (0-80 μM) have been recorded (Fig.8.12). The addition of increasing aliquots of the C4 caused quenching of fluorescence of the DNA-dapi solution which was conclusive of the fact that **C4** could replace DAPI and itself get bound to the minor grooves of DNA. Similar results were obtained for **C5** & **C6**. Thus it can be concluded complexes **C4–C6** prefer groove binding.

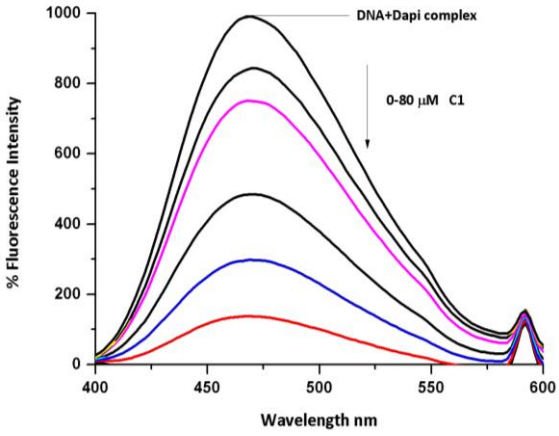

Fig 8.12 : Emission titration of DNA-Dapi complex with increasing concentration of **C4** (0-80 μM)

8.4.2.4 Fluorescence spectral properties of the complexes.

In the emission spectra, all the three complexes (**C4-C6**) displayed emission bands at 470 nm at room temperature when excited at 290 nm.

8.4.2.4.1 Fluorescence probe for DNA detection

Optimization of assay conditions

The effects of pH, concentration of the complex, and reaction time on the detection of ct-DNA were determined. Fluorescence was highest over the pH range of 6–9, and pH 7.2 was used to simulate physiological conditions. Equilibrium was reached within 10 min. The optimum assay conditions were as follows: C1 = 6.6 μg/ml, pH = 7.2, and T= 10 min.

The emission spectrum of **C1** in the presence of varying amounts of DNA is depicted in Fig. 8.13(a). Upon addition of CT DNA to **C4**, the fluorescence intensity gradually increased with no apparent change in the shape and position of the emission bands which implied that the complexes strongly interact with DNA. The hydrophobic environments inside the DNA helix reduces the accessibility of solvent water molecules to **C4** and its mobility was restricted at the binding site, which lead to decrease of relaxation and hence increase in fluorescence intensity [41]. Similar results were obtained for **C5** and **C6**. The binding constant values K, for **C4-C6** were determined from the Scatchard equation [41] and found to be $8.2x10^5\ M^{-1}$, $6.5x10^5\ M^{-1}$ and $7.91.15x10^5\ M^{-1}$ respectively.

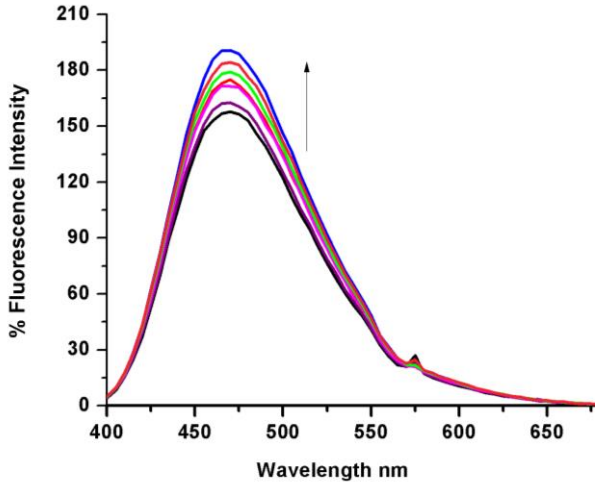

Fig 8.13 (a): Emission spectra of **C4** (6.6 x 10^{-6}M) in the presence of DNA (0-200 x 10^{-6} M) in 5 mM Tris-HCl/50 mM NaCl buffer. Arrows show the intensity changes upon increasing concentration of the DNA.

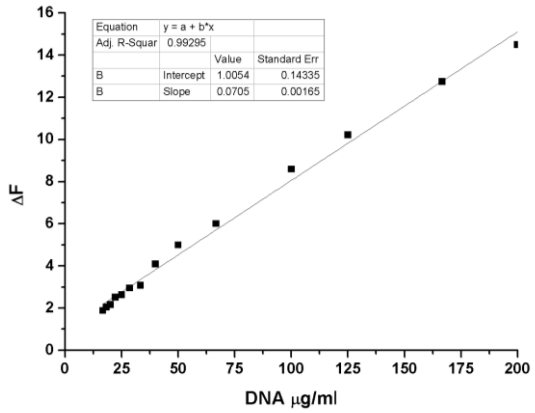

Fig 8.13(b): Calibration graphs for ct-DNA (0-200 x 10^{-6} M)

DNA calibration curve

The fluorescence spectra of **C4** in the presence of DNA is shown in Fig. 8.13(a). The fluorescence intensity was significantly enhanced when the concentration of DNA increased. Moreover, there is a good linear relationship between changes in fluorescence intensity variation (ΔF) and [DNA] (Fig. 8.13(b)), and the linear range of the assay was 0.0–200 μg/ml. The LOD of the assay was calculated from the equation:

$$LOD = 3S_b/m$$

Where S_b is the standard deviation of the blank measurement (n=12) and m is the sensitivity of the calibration curve. The LOD of the **C4**, **C5** and **C6** was determined to be 14.1, 21.6 and 18.2 μg/ml respectively. The sensitivity of our methods is higher compared with many other probes [42]. **C5**-**C6** offers the distinct advantage of easy and economical synthesis and is less toxic compared with some common luminescence probes for nucleic acid determination [42].

8.5 Conclusion

Three novel mixed ligands complexes of VO^{2+}, (**C1-C3**) with the ligands moxifloxacin and dipeptides have been synthesised and studied as selective probes for Cu^{2+} ions. The complexes emit at 450nm on excitation at 288/293nm. Presence or addition of Cu^{2+} show quenching of fluorescence intensity of the complexes due to replacement of VO^{2+} ion from the complexes and formation of Cu(II) mixed ligand complexes as evident from ESI mass spectrometry and IR spectral studies. The quenching of fluorescence is attributed to electron and/or energy transfer from the excited MFL ligand to the non-excited Cu^{2+}ion. The present study demonstrated that mixed ligand vanadyl complexes (**C1-C3**) of dipeptides can be used as chemosensors for selective detection of Cu(II).

Mixed ligands complexes of Zn^{2+},(**C4-C6**) with the ligands moxifloxacin and dipeptides have been synthesised and studied as selective probes for DNA. The DNA binding of **C4-C6** was mediated mainly by groove binding. Moreover, **C4-C6** serves as a sensitive probe for detecting DNA over a wide concentration range with LOD of 14.1 21.6 and 18.2 μg/ml respectively. Therefore, **C4-C6** can be used as a selective probe for DNA detection.

References

[1] Y. Yamaguchi, W. Ding, C.T. Sanderson, M.L. Borden, M.J. Morgan, C. Kutal, Coord. Chem. Rev., 251 (2007) 515.

[2] K.M.-C. Wong, V.W.-W. Yam, Coord. Chem. Rev., 251 (2007) 2477.

[3] K.E. Augustyn, E.D.A. Stemp, J.K. Barton, Inorg. Chem., 46 (2007) 9337.

[4] S.R. Forrest, M.E. Thompson, Chem. Rev., 107 (2007) 923.

[5] Q. Zhao, F. Li, C. Huang, Chem. Soc. Rev., 39 (2010) 3007.

[6] J. Zhao, S. Ji, W. Wu, W. Wu, H. Guo, J. Sun, H. Sun, Y. Liu, Q. Li, L. Huang, RSC Adv., 2 (2012) 1712.

[7] G. Zhou, W.-Y. Wong, X. Yang, Chem. Asian J., 6 (2011) 706.

[8] B. Happ, A. Winter, M.D. Hager, U.S. Schubert, Chem. Soc. Rev., 41 (2012) 2222.

[9] J. Kalinowski, V. Fattori, M. Cocchi, J.A.G. Williams, Coord. Chem. Rev., 255 (2011) 2401.

[10] Y. You, S.Y. Park, Dalton Trans., (2009) 1267.

[11] V.W.-W. Yam, K.M.-C. Wong, Chem. Commun., 47 (2011) 11579.

[12] Q. Zhao, C. Huang, F. Li, Chem. Soc. Rev., 40 (2011) 2508.

[13] P.A. Vigato, V. Peruzzo, S. Tamburini, Coord. Chem. Rev., 256 (2012) 953.

[14] X. Wang, Z. Liu, F. Qian, W. He, Inorg. Chem. Commun., 15 (2012) 176.

[15] S. Basoglu, M. Parlayan, H. Ocak, H. Kantekin, M. Ozdemir, U. Ocak, J. Fluoresc., 19 (2009) 655.

[16] Y. Jeong, J. Yoon, Inorg. Chim. Acta., 381 (2012) 2.

[17] J.F. Zhang, Y. Zhou, J. Yoon, J.S. Kim, Chem. Soc. Rev., 40 (2011) 3416.

[18] J.W. Lichtman, J.A. Conchello, Fluorescence microscopy, Nat. Methods., 2 (2005) 910–919.

[19] (a) P.G. Jiang, L.Z. Chen, J. Lin *et al.* Chem. Commun., (2002) 1424–1425; (b) Q. He, E.W. Miller, A.P. Wong, C.J. Chang, J. Am. Chem. Soc., 128 (2006) 9316.

(c) S. Yoon, E.W. Miller, Q. He, P.H. Do, C. J. Chang, Angew. Chem. Int. Ed., 46 (2007) 6658.

[20] (a) C.-Y. Lai, B. G. Trewyn, D. M. Jeftinija, K. Jeftinija, S. Xu, S. Jeftinija, V. S. Y. Lin, J. Am. Chem. Soc., 125 (2003) 4451.

(b) M. Numata, C. Li, A.-H. Bae, K. Kaneko, K. Sakurai, S. Shinkai, Chem. Commun. (2005) 4655.

[21] (a) D. G. Barceloux, J. Toxicol.-Clin. Toxicol., 37 (1999) 217.

(b) X. B. Zhang, J. Peng, C. L. He, G. L. Shen, R. Q. Yu, Anal. Chim. Acta., 567 (2006) 189.

(c) B. Sarkar, H. Siegel, A. Siegel, Eds.; Marcel Dekker: New York, 12 (1981) 233.

(d)E. L. Que, D. W. Domaille, C. Chang, J. Chem. Rev., 108 (2008) 1517.

[22] P. G. Georgopoulos, A. Roy, M. J. Yonone-Lioy, R. E. Opiekun, P. J. Lioy, J. Toxicol. Environ. Health B., 4 (2001) 341.

[23] Y. Jeong, J. Yoon, Inorg. Chim. Acta., 381 (2012) 2–14.

[24] (a) J. W. Lee, H. S. Jung, P. S. Kwon, J. W. Kim, R. A. Bartsch, Y. Kim, S.-J. Kim, J. S Kim, Org. Lett., 10 (2008) 3801.

(b) K. Kiyose, H. Kojima, Y. Urano, T. Nagano, J. Am. Chem. Soc., 128 (2006) 6548.

(c) E. W. Miller, A. E. Albers, A. Pralle, E. Y. Isacoff, C. J. Chang, J. Am. Chem. Soc., 127 (2005) 16652.

[25] (a) Q. Wu, E. V. Anslyn, J. Am. Chem. Soc., 126 (2004)14682.

(b) Z. Xu, X. Qian, J.Cui, Org. Lett., 7 (2005) 3029.

(c) Y.-Q. Weng, F. Yue, Y.-R. Zhong, B.-H. Ye, Inorg. Chem. 46 (2007) 7749.

[26] S. Neidle, Nucleic Acid Structure and Recognition, Oxford University Press, Oxford, UK, (2002).

[27] C. Yu, K.H.Y. Chan, K.M.C. Wong and V.W.W.Yam, Proc. Natl. Acad. Sci. U. S. A., 103 (2006) 19652

[28] R. Martnez-Mnˇez and F. Sanceno´n, Chem. Rev., 103 (2003) 4419

[29] J. Olmsted and D. R. Kearns, Biochemistry, 16 (1977) 3647

[30] N. A. O'Connor, N. Stevens, D. Samaroo, M. R. Solomon, A. A. Martı´, J. Dyer, H. Vishwasrao, D. L. Akins, E. R. Kandel and N. J. Turro, Chem. Commun., (2009) 2640.

[31] D. Lung, V.P. Yan, D.S.H. Chan, K.H. Leung, H.Z. He, C.H. Leung, Coordination Chemistry Reviews., 256 (2012) 3087.

[32] E. M. Zoupa, S. P. Perlepes, V. Hondrellis, J. M. Tsangaris, J. Inorg. Biochem., 55 (1994) 217.

[33] P.R. Reddy, N. Raju, B. Satyanarayana, Chem. Biodiv., 8 (2011) 131.

[34] J. Dehand, J. Jordanov, F. Keck, A. Mosset, J.J. Bonnet, J. Galy. Inorg. Chem., 18 (1979) 1543.

[35] R. Singh, R. N. Jadeja, M. C. Thounaojam, T. Patel, R.V. Devkar, D. Chakraborty, Inorganic Chemistry Communications, 23 (2012) 78.

[36] G. R. Hanson, T. A. Kabanos, A. D. Keramidas, D. Mentzafos , A. Terzis, Inorg. Chem., 31 (1992) 2587.

[37] N.D. Chasteen In: Berliner L, Reuben J (eds) Biological magnetic resonance, vol. 3. Plenum, New York, (1981) pp 53.

[38] G. Micera, V. L. Pecoraro and E. Garribba , Inorg. Chem., 48 (2009) 5790.

[39] M. Mathieu, P. Van Der Voort, B.M. Weckhuysen, R.R. Rao, G. Catana, R.A. Schoonheydt, E.F. Vansant, J. Phys. Chem. B., 105 (2001) 3393.

[40] J.L. Li, K. Zhang, X.J. Zhang, K.W. Huang, C.Y. Chi, J.S. Wu, J. Org. Chem., 75 (2010) 856.

[41] S.Eriksson, S.K. Kim, M. Kubista, B. Norden, Biochemistry., 32 (1993) 2987.

[42] R. R. Duan, L. Wang, W. Huo, S. Chen, X. Zhou, Spectrochimica Acta Part A: Molecular and Biomolecular Spectroscopy., 128 (2014) 614.